

mined by measuring the peak energy of three narrow resonances which lay in the range 3.5 to 8.2 Mev as a function of gas pressure. These peak energies were then extrapolated to zero pressure. The correction varied from 0.018 to 0.003 Mev.

Comparison with the most recent Rice University data⁵ indicates a systematic cross-section difference of about 5% with our work. The original data taken by Henry fit our data slightly better than the later data taken at Rice. Figure 4 shows this comparison at the respective back angles. The Rice data are plotted as circles and crosses and our data as a solid line. Rice data do not show the narrow satellite level at 5.402 Mev which has been identified as s_3 .³

Work done by Sempert, Schneider, and Martin⁷ is compared to ours at the two nearly equal angles. The agreement is not good. Their results are consistently high an amount several times their quoted uncertainty of $\pm 10\%$. The comparison is shown in Fig. 4.

Kobayashi's work⁶ is compared to ours in the cases for which we have data at comparable angles. See Fig. 5. Agreement is excellent, cross sections usually agreeing within the combined experimental uncertainties. Kobayashi estimates his uncertainty as a few millibarns, and ours is about $\pm 0.5\%$. The experimental resolution is much poorer for Kobayashi's work than for ours so his data would be expected to agree with ours only in regions of slowly varying cross section.

F¹⁷ Level Parameters*

S. R. SALISBURY† AND H. T. RICHARDS
University of Wisconsin, Madison, Wisconsin
 (Received February 1, 1962)

O¹⁶(p,p)O¹⁶ differential cross-section data for $E_p=2-7.6$ Mev have been used to fix parameters of F¹⁷ levels. The cross-section data were first fitted to a partial-wave phase-shift expansion by a least-squares method using an IBM 704. The level parameters were then obtained by application of dispersion formalism to the extracted phase shifts. The two-level approximation was used where appropriate. Four very narrow levels and the well-known $7/2^-$ level at $E_p=3.47$ Mev were ignored in the present analysis. However, resonant energies and limits on widths (obtained by inspection) for these and higher energy F¹⁷ states are given. Level schemes of O¹⁷ and F¹⁷ are compared. Assignment of levels to particular nuclear configurations is attempted. An appendix is included, giving illustrations of branching solutions in the phase-shift analysis.

INTRODUCTION

SUCCESSFUL analysis of O¹⁶(p,p)O¹⁶ data will fix level parameters in the compound nucleus F¹⁷. Differential cross sections for this interaction in the proton energy range from 4.25 to 8.6 Mev are reported in the preceding paper.¹ These cross sections are used for the phase-shift analysis in the range $E_p=4.25-7.6$ Mev. Data taken by Eppling² at Wisconsin, and by groups at Rice University^{3,4} are here used for a similar analysis in the range $E_p=2.0-4.25$ Mev.

Dispersion formalism permits the reproduction of each resonant phase shift by a set of level parameters. The present analysis stops with the extraction of such level parameters. A logical further step would be the generation of these level parameters by a simple nuclear model.

* Work supported by the U. S. Atomic Energy Commission, and by the Graduate School from funds supplied by the Wisconsin Alumni Research Foundation.

† Present address: Missile and Space Division, Lockheed Aircraft Corporation, Palo Alto, California.

¹ S. Salisbury, G. Hardie, L. Oppliger, and R. Dangle, preceding paper [Phys. Rev. **126**, 2143 (1962)].

² F. Eppling, Ph.D. thesis, University of Wisconsin, 1952 (unpublished).

³ R. W. Harris, Rice University (private communication).

⁴ R. R. Henry, G. C. Phillips, C. W. Reich, and J. L. Russell, Bull. Am. Phys. Soc. **1**, 96 (1956).

THE PHASE-SHIFT ANALYSIS

The partial wave expansion takes the following form for the case of spin- $\frac{1}{2}$ particles on spin-zero particles.^{5,6} (The notation follows reference 6.)

$$d\sigma/d\Omega(\text{c.m.}) = (1/k^2)(|A|^2 + |B|^2),$$

where

$$A = -\frac{1}{2}\eta \csc^2(\theta/2) \exp i\eta \ln[\csc^2(\theta/2)]$$

$$+ \sum_l (l+1) P_l(\cos\theta) \sin\delta_l^+ \exp i(\alpha_l + \delta_l^+)$$

$$+ \sum_l l P_l(\cos\theta) \sin\delta_l^- \exp i(\alpha_l + \delta_l^-),$$

$$B = \sin\theta \sum_l \frac{dP_l(\cos\theta)}{d \cos\theta} [\sin\delta_l^- \exp i(\alpha_l + \delta_l^-)$$

$$- \sin\delta_l^+ \exp i(\alpha_l + \delta_l^+)].$$

The preceding expression is valid if the elastic scattering channel is the only open channel. If one neglects the small (p,γ) widths, then up to $E_p=5.55$ Mev only the elastic scattering channel is open. At $E_p=5.55$ Mev, the O¹⁶(p,α)N¹³ channel opens. At $E_p=6.3$ Mev, the O¹⁶(p,p')O^{16*} channel opens. If these

⁵ C. L. Critchfield and D. C. Dodder, Phys. Rev. **76**, 602 (1949).

⁶ R. A. Laubenstein and M. J. W. Laubenstein, Phys. Rev. **84**, 18 (1951).

reactions should have reduced widths near the Wigner limit, their influence (for low- l waves) might become appreciable a few hundred keV above their thresholds. Hence, our phase-shift analysis may be questionable at the higher energies. However, the fact that reasonable phase shifts result from our simple formula at the higher energies may indicate that our neglect of these open channels is not serious.

Extraction of Level Parameters

In relating the extracted phase shifts to resonant parameters, we distinguish two cases:

(a) The "one-level" approximation⁷⁻⁹: Over the range of a resonance, no other resonance of the same

J and parity has appreciable amplitude. For this case

$$\delta_i^\pm = \beta_i^\pm + \phi_i^\pm,$$

$$\beta_i^\pm = \tan^{-1} \left(\frac{k\gamma_\lambda^2/A_i^2}{E_\lambda + \Delta_\lambda - E} \right)_a.$$

The level shift Δ_λ is negligible for narrow levels and its actual form depends on certain boundary conditions. The form used here, $\Delta_\lambda = -k\gamma^2(F_l/A_i^2 G_l)_a$, results from the boundary conditions assumed by Sachs⁷ and Teichmann and Wigner.⁸ It differs from an earlier form used by Wigner and Eisenbud⁹ and Thomas.¹⁰

(b) The "two-level" approximation: Over the range of a resonance another resonance of the same J and parity has appreciable amplitude. Then,

$$\beta_i^\pm = \tan^{-1} \left(\frac{(k/A_i^2)_a}{[\gamma_{\lambda 1}^2/(E_{\lambda 1} - E) + \gamma_{\lambda 2}^2/(E_{\lambda 2} - E)]^{-1} - (kF_l/A_i^2 G_l)_a} \right),$$

where the subscripts 1 and 2 denote the two levels involved. This formula differs slightly from that given by Adair,¹¹ because he used the earlier boundary condition.

STRUCTURE OF COMPUTER PHASE-SHIFT PROGRAM

The cross sections above $E_p = 3.5$ Mev display a complicated structure. Therefore, it was felt a graphical analysis was impractical. Instead, an IBM 704 was programmed for a phase-shift analysis.¹²

This program uses an initial set of phase angles,

$$\delta_0^+, \delta_1^+, \delta_1^-, \delta_2^+, \delta_2^-, \delta_3^+, \delta_3^-,$$

at some energy E to calculate differential cross sections for the eight angles of observation. (The subscript is the l value of the partial wave and the superscript is \pm as $J = l \pm \frac{1}{2}$.) The program compares these cross sections with the experimental cross sections in terms of an error function of the form:

$$\chi^2 = \sum_{i=1}^8 \left(\frac{(d\sigma/d\Omega)_{\text{exp}_i} - (d\sigma/d\Omega)_{\text{cal}_i}}{\epsilon_i} \right)^2,$$

where

$$\epsilon_i = [0.015(d\sigma/d\Omega)_{\text{exp}_i} + 0.1] \text{ mb/sr}$$

is the assigned experimental error and i indicates the experimental angle of observation.

⁷ R. G. Sachs, *Nuclear Theory* (Addison-Wesley Publishing Company, Cambridge, 1953), p. 290.

⁸ T. Teichmann and E. P. Wigner, *Phys. Rev.* **87**, 123 (1952).

⁹ E. P. Wigner and L. Eisenbud, *Phys. Rev.* **72**, 29 (1947).

¹⁰ R. G. Thomas, *Phys. Rev.* **81**, 148 (1951).

¹¹ R. K. Adair, quoted as a private communication by: A. Galonsky and M. T. McEllistrem, *Phys. Rev.* **98**, 590 (1955).

¹² Complete Fortran listings and descriptions of all the programs discussed in this paper with sample input-output data are in the Ph.D. thesis of S. R. Salisbury, University of Wisconsin, 1962 (unpublished). This thesis is available through University Microfilms, Ann Arbor, Michigan.

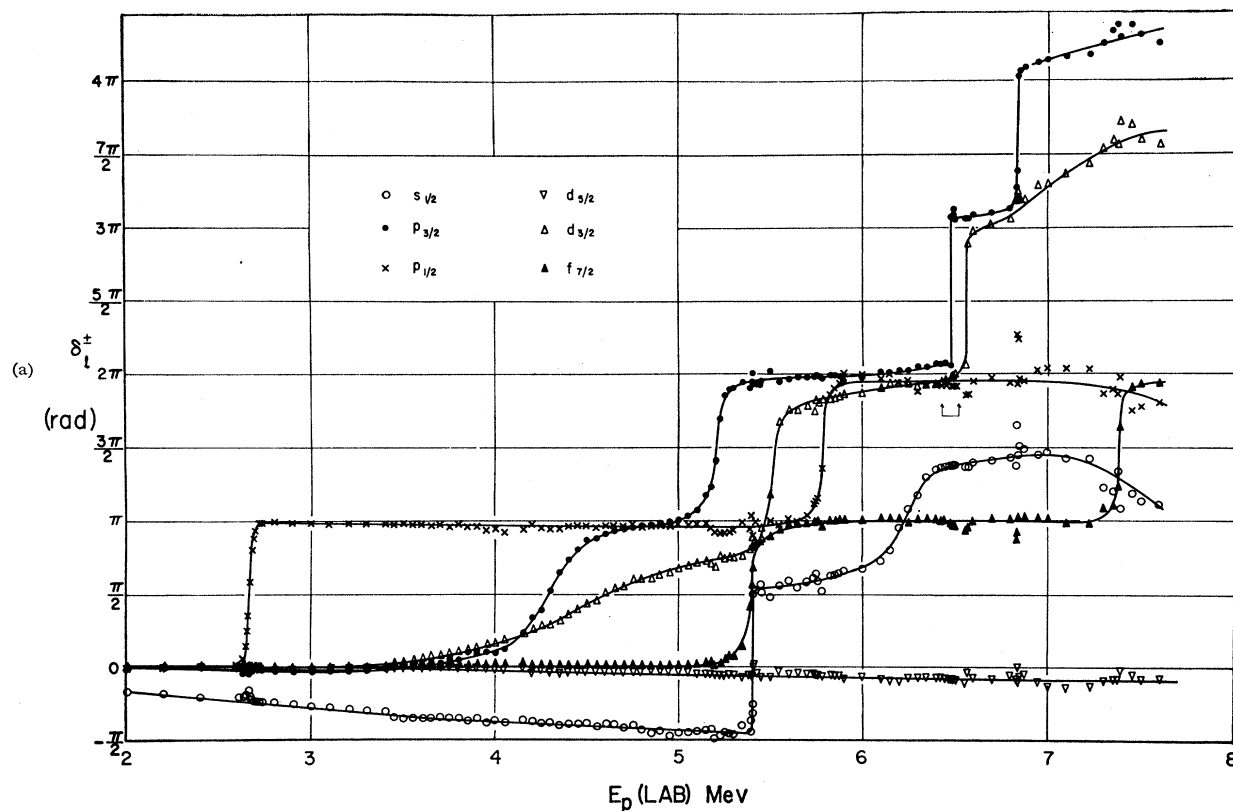
The phase angle δ_0^+ is first varied until a minimum in χ^2 is found. Then, δ_0^+ is fixed at this value, and δ_1^+ is varied until again a minimum in χ^2 is found. This procedure is repeated for all the phase angles. The final value of χ^2 is termed the error at the end of the first cycle. These cycles are repeated until the change in χ^2 per cycle is less than a specified amount. The set of phase angles resulting in this final χ^2 is then termed the best set resulting from the particular initial set chosen. A $\chi^2 = 8$ corresponds to a fitting within the assigned uncertainty ϵ .

Several subroutines were used to carry solutions to higher energies. For preliminary investigation of all resonance regions, solutions were first obtained at either end of the region. Then, the machine was programmed to find solutions at various energies within the region, letting only a few of the phase angles be free search variables, the others varying linearly between the two known solutions. This technique approximates the physical situation in a resonance region when only one, or at most several, of the phase angles are resonant (i.e., changing relatively rapidly). It also saves on computer time.

These approximate solutions were used at intermediate energies as initial sets for searches in which all parameters are free search variables.

Since the data at the eight scattering angles have $\sim 1\%$ uncertainty, and employ at least six phase angles as parameters, it is usually possible to get several solutions at a given energy which fit the data equally well. Two arguments are used to select the correct set of phase angles:

(a) The analysis is begun at a sufficiently low energy ($E_p = 2$ Mev) that apart from the Rutherford term, only the s wave should have appreciable amplitude.



Thus, the only physically plausible solution is one with only the s phase shift large.

(b) A physically correct set of phase shifts must be continuous. If phase-shift fittings are made at sufficiently small intervals, we can reject any set with abrupt phase changes as long as no abrupt changes in cross section occur.

In addition, Wigner¹³ shows that $d\delta/dE \geq -A$, where A is a positive number which is an explicit function of l and the interaction radius. This criterion was used in a few places to exclude solutions.

RESULTS FROM COMPUTER PHASE-SHIFT PROGRAM

A solution was found at $E_p = 2$ Mev satisfying the physical arguments mentioned earlier. It also agreed well with a set of phase shifts extracted graphically by Eppling² at this energy. Solutions were then found at $E_p = 2.2, 2.4, 2.6, 2.73$ Mev, and every 100 keV thereafter to 3.4 Mev. Fitting of the first resonance is described in detail, subsequent fittings are only briefly commented upon unless there occurred unusual difficulties. Resulting phase shifts are shown in Fig. 1(a), χ^2 in Fig. 1(b), and comparisons of calculated and experimental cross sections in Figs. 2, 3, and 4.

¹³ E. Wigner, Phys. Rev. **98**, 145 (1955).

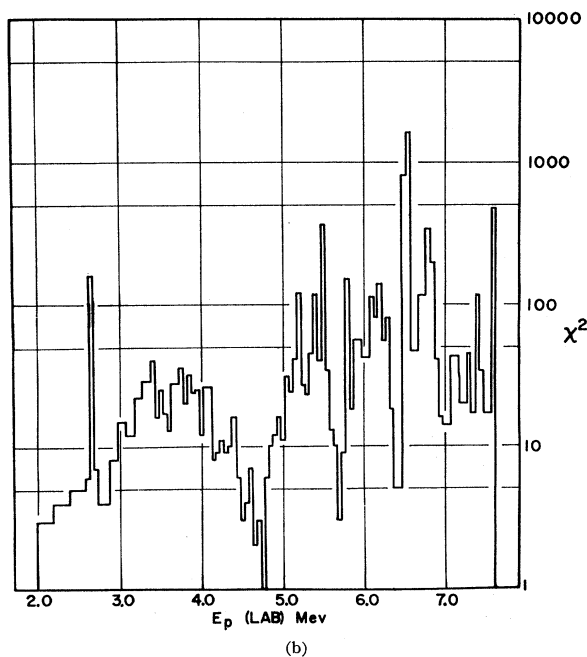


FIG. 1. (a) Extracted phase shifts δ_l^\pm for the reaction $O^{16}(p,p)O^{16}$ in the incident-proton energy range 2 to 7.6 Mev. $J = l \pm \frac{1}{2}$. (The region indicated within the arrows around 6.5 Mev was only investigated with single parameter variations.) Note that π change in the δ_{s^+} phase corresponding to the well-known very sharp resonance at $E_p = 3.47$ Mev has been omitted. (b) Resulting χ^2 for extracted phases of Fig. 1(a). A fit at all angles to within 1.5% corresponds to a $\chi^2 = 8$.

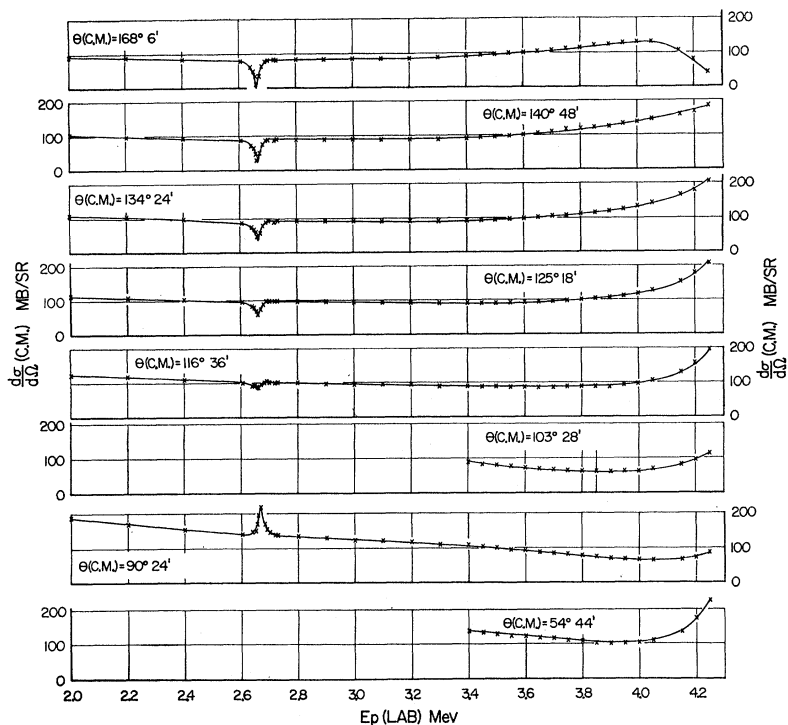


FIG. 2. Comparison of the calculated cross sections (crosses) to the experimental cross sections^{2,4} (solid lines) in the incident-proton energy range 2 to 4.25 Mev. The cross sections are calculated from the phase angles plotted in Fig. 1. (Note: the very narrow resonance at $E_p=3.47$ Mev has been omitted from the figure and the analysis.)

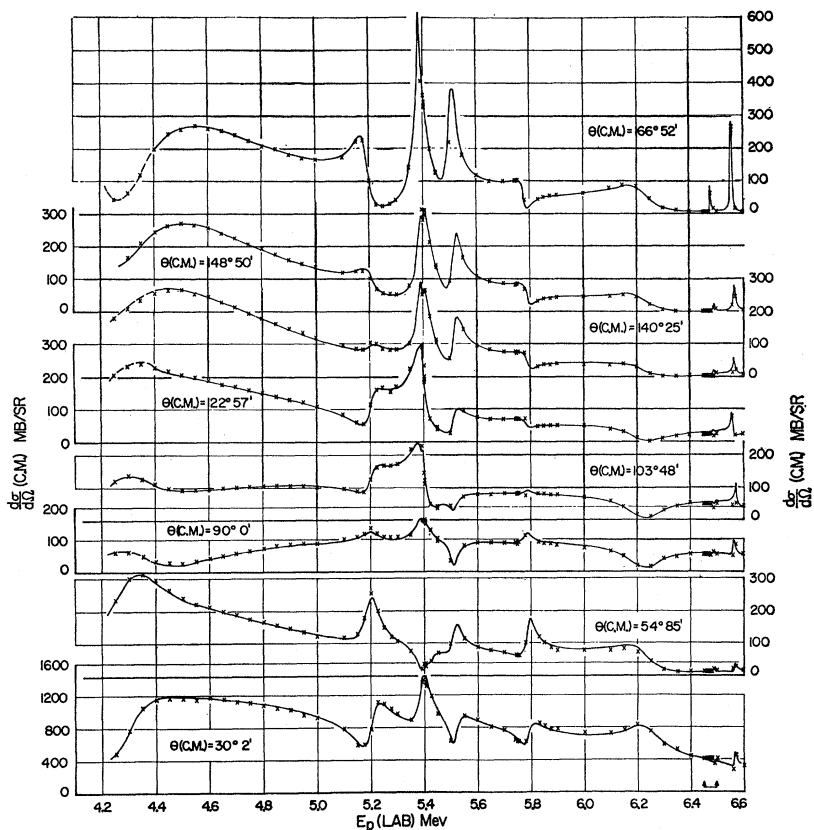


FIG. 3. Comparison of the calculated cross sections (crosses) to the experimental cross sections (solid lines) in the incident-proton energy range 4.25 to 6.6 Mev. The calculated cross sections are obtained from the extracted phase angles in Fig. 1.

Resonance at $E_p = 2.66$ Mev

This resonance is nicely isolated so only one resonant phase shift is expected. The program is asked for solutions at proton energies from 2.6 to 2.73 Mev in steps ranging from 0.020 to 0.003 Mev dependent on rate of change of cross section. One phase shift is free to be varied by the program; the others are linearly varied between their known values, from the previous all-parameter variations at $E_p = 2.60$ and 2.73 Mev. This program was run six times. Each of six phases were presumed resonant in turn. Only the δ_{1^-} went through the characteristic resonant curve. Then, using these approximate sets as initial choices at various energies in the resonant region, all parameter fittings were made. These are the final extracted phase shifts plotted in Fig. 1. The $1/2^-$ assignment for the $E_p = 2.66$ anomaly agrees with that found by Eppling.²

The narrow $7/2^-$ resonance at $E_p = 3.47$ Mev was not reinvestigated here, because its assignment was not in question, and since it is very narrow, it makes negligible contribution to the δ_{3^+} phase shift for protons 0.050 Mev away. Thus, it doesn't appreciably interfere with

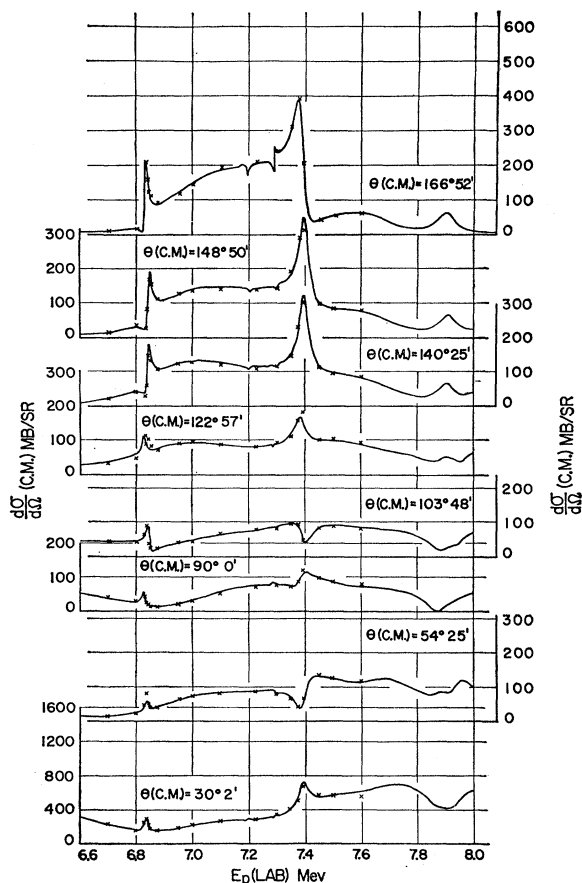


FIG. 4. Comparison of the calculated cross sections (crosses) to the experimental cross sections (solid lines) in the incident-proton energy range 6.6 to 7.6 Mev. The calculated cross sections are obtained from the extracted phase angles of Fig. 1.

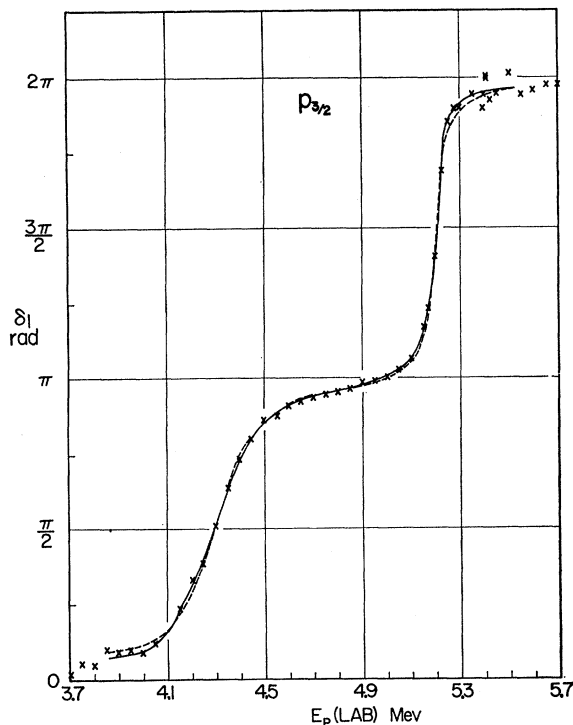


FIG. 5. Comparison of the experimental phase angle δ_{1^+} (crosses) to the phase angle $\beta_{1^+} + \phi_{1^+}$ (dashed line) which is calculated from the two-level approximation using the level parameters of Table I. The calculated curve is dashed and the solid line is a freehand smooth curve used in the program for fitting.

our finding a continuous set of phase shifts through this region.

Two Broad Resonances for Protons between 4 and 5 Mev

The analysis here was difficult and it provides a good example of branching solutions. The reasons for choosing a particular branch are discussed in detail in the appendix. To identify the levels and get approximately correct sets of phase shifts, a two-parameter variation was done. Here, any two phase shifts are presumed resonant and varied by the program. The others are varied linearly with energy between known solutions at either end of the resonant region. This method is difficult to use, because these resonances are very broad and, hence, produce strong effects all the way from 3.6 to 5 Mev. The set at 3.6 Mev is well known from its continuity with solutions at lower energies. However, from the many sets which can be found at 5 Mev the correct set cannot easily be singled out without having identified the intervening resonances. Nevertheless, using variations of the previously discussed techniques, it was possible to identify the levels. Then, all parameter variations were done using the approximate values from the two-parameter variations as initial guesses.

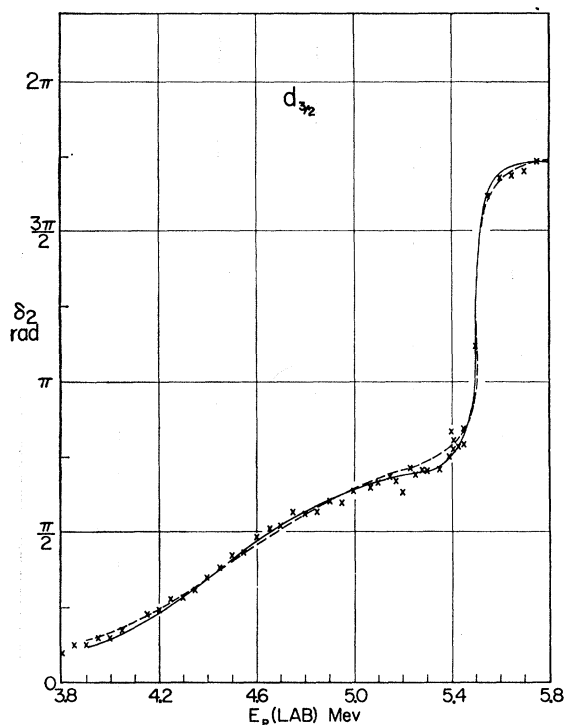


FIG. 6. Comparison of the experimental phase angle $\delta_2^- - \Delta$ (crosses) to the phase angle $\beta_2^- + \phi_2^-$ (dashed line) which is calculated from the two-level approximation using the level parameters of Table I. Δ is the extrapolated value of the resonant phase angle for the $3/2^+$ level at $E_p = 7.3$ Mev.

Resonances at $E_p = 5.23, 5.39, 5.40, 5.55,$ and 5.78 Mev

This region, although complicated, consists of narrow resonances which are sufficiently separated to yield to straight forward treatment.

The most difficult region is the peak at $E_p = 5.40$ Mev which was shown to arise from two levels, a moderately narrow $7/2^-$ with a very narrow $1/2^+$ superimposed. The $1/2^+$ is not cleanly resolved and, so, was hard to identify. Levels at $E_p = 5.23$ and 5.55 Mev, which were shown to be $3/2^-$ and $3/2^+$, respectively, are noteworthy in that they occur close enough to the broad $3/2^-$ and $3/2^+$ found at lower energies to interfere with them.

The resonance at $E_p = 5.78$ Mev was easily identified as $1/2^-$. At some angles, there is a suggestion of another level which may account for scatter in the extracted δ_0^+ and δ_3^+ phases.

Resonance at $E_p = 6.33$ Mev

This broad resonance was hard to identify as there are many solutions near each other (see appendix for discussion of branching solutions in this region). However it was finally shown to be clearly a $1/2^+$ level.

Competing reactions may well start to be important here. Inelastic scattering has its threshold at $E_p = 6.3$ Mev, and the $O^{16}(p, \alpha)N^{13}$ reaction threshold is at

$E_p = 5.55$ Mev. Because of these opening channels our phase-shift analysis may become gradually of less significance.

Resonances at $E_p = 6.48$ and 6.58 Mev

The resonance at $E_p = 6.483$ Mev is sufficiently resolved to be identified as $3/2^-$, but the fits are not too good. The final phase shifts shown between the arrows in Fig. 1 and Fig. 3 are single parameter fittings, which are all that the data justified.

The resonance identified as $3/2^+$ at 6.584 Mev was assigned by straight forward techniques.

Resonance at $E_p = 6.83, 7.3,$ and 7.39 Mev

The levels at 6.83 and 7.39 Mev were identified as $3/2^-$ and $7/2^-$, respectively, in the usual manner. However, a large scatter is found in the nonresonant phase shifts over these regions. This scatter may again reflect the need for considering the other open channels and perhaps higher order partial waves.

A very broad level identified as $3/2^+$ is found at 7.313 Mev which produces strong effects down to 6 Mev. There is evidence for the start of a very broad $3/2^-$ resonance in this same region, but the analysis was not carried up to a high enough energy to make a positive identification.

The analysis was stopped at this point, because the increasing lack of precision in fitting did not justify more machine time.

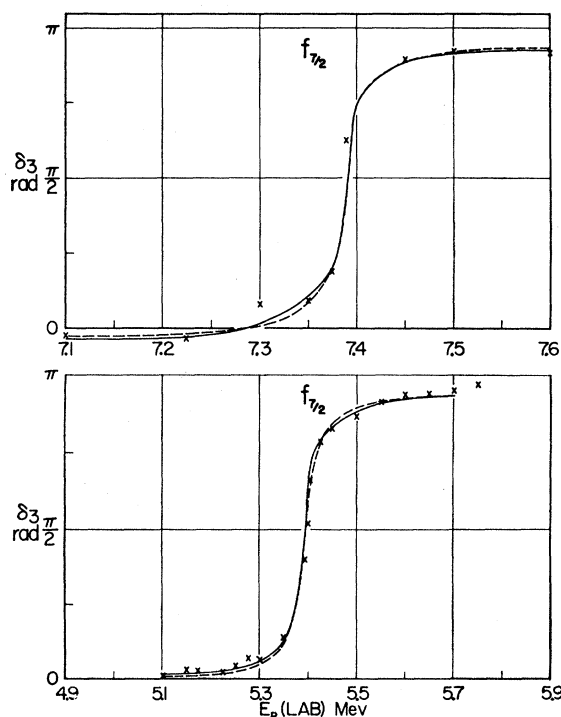


FIG. 7. Comparison of the experimental phase angle δ_3^+ (crosses) to the phase angle $\beta_3^+ + \phi_3^+$ (dashed line), which is calculated (in the one-level approximation) using the level parameters of Table I.

STRUCTURE OF COMPUTER LEVEL
PARAMETER PROGRAM

This program generates a phase-shift curve from the level parameters of either a single isolated resonance or two interfering resonances. This curve is compared by the program to a free-hand smooth curve. This latter curve is shown in Figs. 5 through 10 as the solid line through the experimental phase shifts. The program then varies the level parameters so as to produce a minimum least-squares error.

The comparison is made point by point between 48 points taken from the smooth curve mentioned above, and an equal number of points calculated from the level parameters. The error is calculated in terms of the formula:

$$\chi^2 = \sum_{i=1}^{48} [\beta_i^\pm(E_i)_{\text{cal}} + \phi_i^\pm - \delta_i^\pm(E_i)_{\text{exp}}]^2,$$

where $\delta_i^\pm(E_i)_{\text{exp}}$ are phases at E_i as read from a smooth curve through the extracted phase angles of Fig. 1; $\beta_i^\pm(E_i)_{\text{cal}}$ are the resonant phase shifts calculated at E_i from either the one- or two-level approximation, and ϕ_i^\pm is an adjustable potential phase assumed constant for a given energy region.

Originally, in place of $\phi_i = \text{constant}$, we used the hard-sphere phase shifts, $\phi_i = -\tan(F_i/G_i)_0$. It was found that the nonresonant part of the extracted phase shifts did not agree well with this when using a reasonable value of interaction radius a .

Teichmann and Wigner suggest⁸ that instead of using

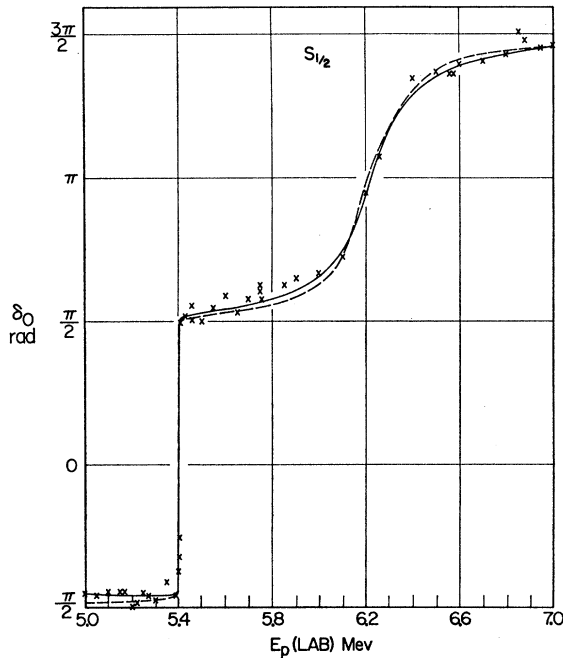


FIG. 8. Comparison of the experimental phase angle δ_0^+ (crosses) to the phase angle $\beta_0^+ + \phi_0^+$ (dashed line) which is calculated from the two-level approximation, using the level parameters of Table I (but with F_0/G_0 replaced by F_1/G_1 , see text).

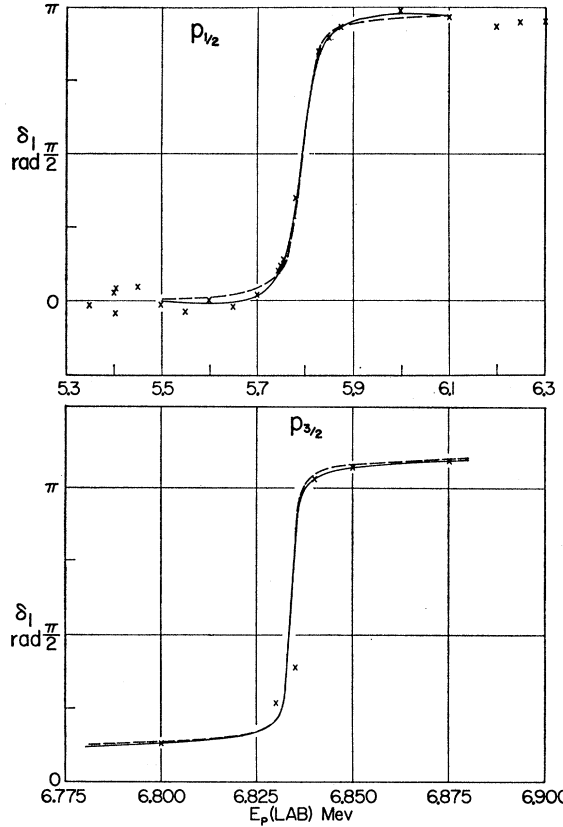


FIG. 9. The upper half shows a comparison of the experimental phase angle δ_1^- (crosses) to the phase angle $\beta_1^- + \phi_1^-$ (dashed line) calculated (in the one-level approximation) using the level parameters of Table I. The lower half shows the same comparison for the experimental phase angle δ_1^+ and the calculated phase angle $\beta_1^+ + \phi_1^+$.

F_i/G_i as the argument of \tan^{-1} , a function varying quite slowly with energy should be used. The value of the function should be that which allows best fitting of the experimental data.

It was decided to assume that ϕ_i^\pm was constant over the energy interval considered in one fitting. This constant was adjusted for each resonance to yield the best fit.

The same logic was used in this program as in the phase-shift analysis, one cycle being a variation of each of the parameters until a minimum is reached. The cycles were continued until the rate of convergence of χ^2 was less than a specified amount.

RESULTS FROM THE LEVEL
PARAMETER PROGRAM

Initial resonant energy and width parameters were chosen by inspection of the curves; however, the search would converge to a unique solution even with an obviously poor initial set of parameters.

The deduced level parameters corresponding to all the analyzed levels are shown in Table I. The free-hand

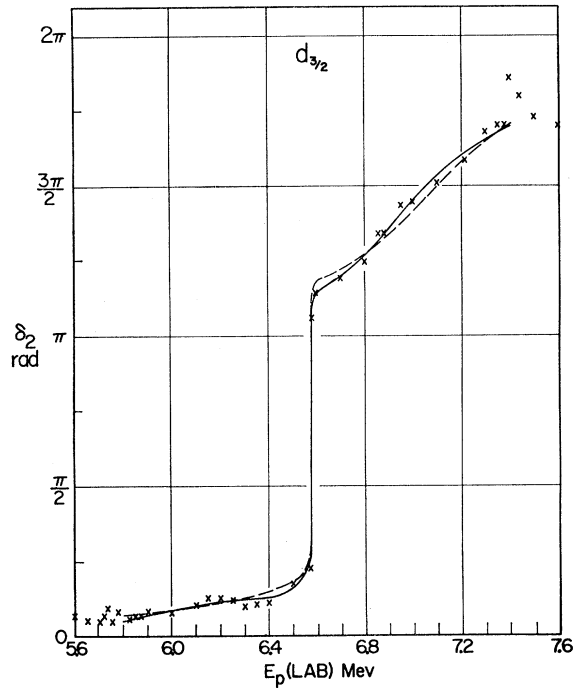


FIG. 10. Comparison of the experimental phase angle $\delta_{3/2} - \Delta$ (crosses) to the phase angle $\beta_{3/2} + \phi_{3/2}$ (dashed line) calculated from the two-level approximation using the level parameters of Table I. Δ is the extrapolated value of the resonant phase angles for the $3/2^+$ levels at $E_p = 4.79$ and 5.55 Mev.

smooth curves through the extracted resonant phase shifts and the dashed curves calculated from the level parameters of Table I are shown in Fig. 5 through 10. Special comment is necessary concerning a few cases:

(a) Figure 6. The interfering $3/2^+$ levels at $E_p = 4.787$ Mev and $E_p = 5.546$ Mev. The broad $3/2^+$ level at $E_p = 7.3$ Mev has appreciable effects in this region, so a three-level approximation is really indicated. However, the two-level approximation was already sufficiently complex and the phase shifts at higher energies uncertain enough that only the simpler assumption of additivity of the phase shifts from the $E_p = 7.3$ Mev level was used.

A preliminary fitting of the $3/2^+$ level at 7.31 Mev was made and the resulting phase angles extrapolated to $E_p = 3.9$ Mev. Values of these extrapolated angles were subtracted from the extracted phase shifts for the $3/2^+$ levels at $E_p = 4.79$ and 5.55 Mev. The resulting phase shifts are shown as crosses in Fig. 6. It can be seen from this figure that a two-level approximation for the residual phases is reasonably satisfactory.

(b) Figure 8. The interfering $1/2^+$ levels at $E_p = 5.402$ Mev and $E_p = 5.332$ Mev. Straight forward application of the two-level dispersion formalism to extract the level parameters for these levels gave nonsensical results. The difficulty was finally traced to the fact that the level shift contained F_0/G_0 as a factor. In this energy region and for our assumed interaction, radius

TABLE I. Parameters^a for F^{17} levels.

Assign. J^π	E_λ (lab) ^b (Mev)	γ^2 ^c (Mev cm)	Γ (lab) ^c (Mev)	$\left(\frac{\gamma^2}{3} \frac{\hbar^2}{2\mu a}\right)$ ^c	$E_x(F^{17})$ ^d (Mev)	E_r ^e (Mev)	ϕ_{I^\pm} (radians)
1/2 ⁻	2.66 ^f	0.109×10^{-13}	0.020 ^f	0.840×10^{-2}	3.10 ^f	2.66 ^f	
7/2 ⁻	3.47 ^f	$\leq 0.258 \times 10^{-13}$	≤ 0.003 ^f	$\leq 0.19 \times 10^{-1}$	3.86 ^f	3.47 ^f	
3/2 ⁻	4.354	0.548×10^{-13}	0.240	0.424×10^{-1}	4.694	4.304	0.075
3/2 ⁺	4.787	0.645×10^{-12}	1.63	0.506	5.101	4.672	0.000
3/2 ⁻	5.231	0.132×10^{-13}	0.0725	0.102×10^{-1}	5.519	5.210	0.075
7/2 ⁻	5.392	0.456×10^{-13}	0.0429	0.352×10^{-1}	5.670	5.396	-0.050
1/2 ⁺	5.402	$< 0.110 \times 10^{-15}$	< 0.0006	$< 0.850 \times 10^{-4}$	5.680	5.402	-1.625
3/2 ⁺	5.546	0.586×10^{-13}	0.191	0.452×10^{-1}	5.816	5.514	0.000
1/2 ⁻	5.779	0.491×10^{-14}	0.030	0.395×10^{-2}	6.035	5.792	-0.025
1/2 ⁺	6.332	0.310×10^{-13}	0.216	0.240×10^{-1}	6.556	6.226	-1.625
3/2 ⁻	6.484	$< 0.391 \times 10^{-15}$	< 0.003	$< 0.3 \times 10^{-3}$	6.699	6.484	0.225
3/2 ⁺	6.564	0.918×10^{-15}	0.00480	0.709×10^{-3}	6.774	6.564	0.050
3/2 ⁻	6.833	0.361×10^{-15}	0.00404	0.278×10^{-3}	7.026	6.834	0.400
	7.180		≤ 0.01		7.356		
	7.280		≤ 0.005		7.438		
	7.287		≤ 0.005		7.447		
	7.305		≤ 0.005		7.469		
3/2 ⁺	7.313	0.162×10^{-12}	0.845	0.125	7.479	7.028	0.050
7/2 ⁻	7.385	0.114×10^{-13}	0.0267	0.882×10^{-2}	7.547	7.388	-0.125
	7.625 ± 0.030		0.1		7.766		
	7.875 ± 0.020		0.05		8.008		
	7.940 ± 0.020		0.05		8.057		
	8.275 ± 0.005		0.005		8.386		
	8.310 ± 0.010		0.03		8.418		

^a Interaction radius, $a = 5.10 \times 10^{-13}$ cm.
^b Energies are quoted to four significant figures, because the programs are able to distinguish changes in the 4th place. However, energy shifts in the proton beam make these energies uncertain to ± 0.01 Mev.
^c Three significant figures are quoted in γ^2 and related quantities unless otherwise specified. This is done because the programs are able to distinguish changes at least in the 3rd place. However, the uncertainty in drawing a curve through the extracted phase shifts, especially for levels having < 0.02 Mev, indicates that physically the parameters are not known nearly this well.
^d $E_x(F^{17}) = (16/17)E_\lambda + 0.596$ Mev.
^e E_r is the value of E_p (lab) Mev for which $\beta^\pm = \frac{1}{2}\pi$ (or $\frac{3}{2}\pi$ in the case of interfering levels).
^f Quantities obtained from reference 2 and 6. γ^2 and related quantities are calculated from their quoted Γ .

F_0/G_0 becomes discontinuous. Teichmann and Wigner⁸ point out that the dispersion formalism derived by them, and used here, is only useful when quantities like F_l/G_l vary slowly with energy. So the boundary conditions which give the specific form of level shift used here are probably not appropriate for s waves in this energy region.

However, F_1/G_1 is continuous in this energy interval and is intermediate in value to F_0/G_0 in the regions on either side of the discontinuity. We would like to choose a slowly varying quantity to be used instead of F_0/G_0 in this region, and, hence, it is convenient and reasonable to choose F_1/G_1 . However, to avoid re-

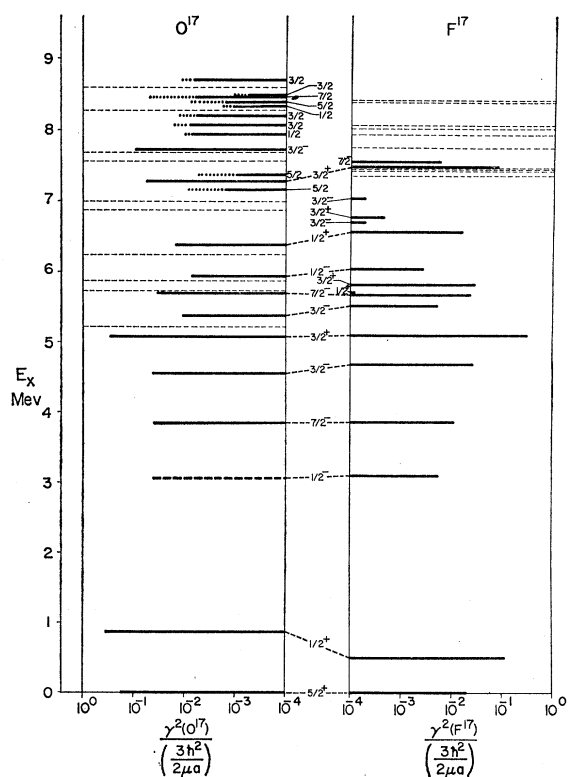


FIG. 11. Comparison of the energy level schemes of O¹⁷ and F¹⁷. For levels having a known J and parity, the length of the solid heavy line indicates on a logarithmic scale the ratio of experimental reduced width to the Wigner limit. For levels having an unknown parity, the length of the solid heavy line and the solid heavy plus dotted line corresponds to the two possible parities. Unidentified levels are indicated by light dashed lines. Reduced widths for levels below $E_x=1$ Mev in F¹⁷ and below $E_x=4$ Mev in O¹⁷ are obtained from stripping reactions. The relative stripping widths for O¹⁷ [T. S. Green and R. Middleton, Proc. Phys. Soc. (London) A69, 28 (1956)] have been normalized to the width (from neutron scattering) of the level at $E_x(O^{17})=4.56$ Mev [C. K. Bockelman, D. W. Miller, R. K. Adair, and H. H. Barschall, Phys. Rev. 84, 69 (1951)]. The stripping widths for F¹⁷ are directly from B. Yaramis, Phys. Rev. 124, 836 (1961) and are not normalized to scattering widths. The $1/2^-$ level in O¹⁷ at $E_x(O^{17})=3.06$ Mev does show stripping behavior so only a limit on θ^2 can be given. The limit here assumed (heavy dashed line) is that observed for the neighboring $7/2^-$ level which does exhibit stripping. Widths for levels in O¹⁷ above $E_x(O^{17})=4$ Mev are from the neutron data. Widths for levels in F¹⁷ above $E_x(F^{17})=1$ Mev are from Table I.

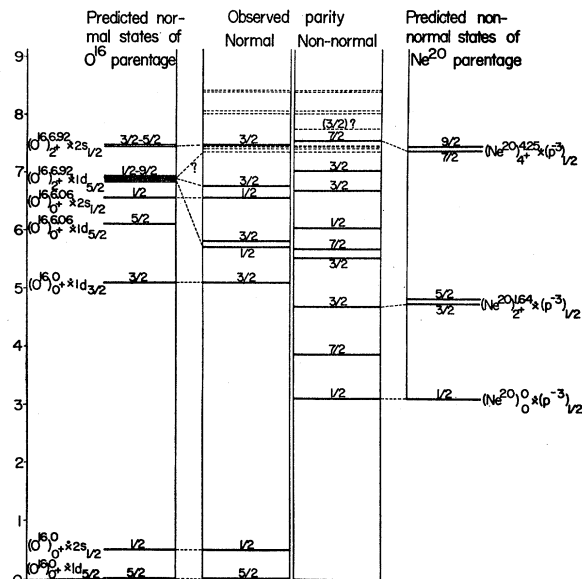


FIG. 12. Possible parentage of some F¹⁷ states. "Normal" parity corresponds to that of F¹⁷ ground state, i.e., even. Dashed lines show levels with unidentified J and parity.

writing the machine program, we are then forced also to use A_1^2 instead of A_0^2 . A_0^2 is well behaved and approximately constant in this region, and it has the form $A_0^2 \approx 0.9A_1^2$. The substitution of A_1^2 for A_0^2 should then produce only a small effect on the extracted parameters. The fit shown in Fig. 8 was obtained in this manner. The reduced widths quoted in Table I, however, have been corrected so that they correspond to the A_0^2 value.

It may be noted that physically $-\tan^{-1}(F_0/G_0)$ corresponds to the phase shift resulting from scattering by a hard sphere surrounded by a Coulomb field. The discontinuous behavior of F_0/G_0 in this region then would correspond to a $s_{\frac{1}{2}}$ "size" resonance.

(c) The $3/2^-$ level at $E_p=6.48$ Mev. The lab width of this resonance, as determined from inspection of the back angle cross section, is ≤ 0.003 Mev. Since our experimental energy resolution is comparable to this width, no machine extraction of level parameters was attempted. However, the resonant energy can still be closely fixed by inspection of the back-angle data, since the resonance energy must lie between the minimum and maximum of the cross section.

(d) Figure 10. The interfering $3/2^+$ levels at $E_p=6.564$ and $E_p=7.313$ Mev. The problems here are similar to the lower pair of $3/2^+$ resonances, and solutions are similar: extrapolated values of the phase shifts from the lower pair were subtracted from the phase shifts used in this fitting.

DISCUSSION

Table I lists the resonant parameters for all the known levels between incident proton energies of 2.66 and 8.31 Mev.

All levels through the $7/2^-$ at $E_p=7.385$ Mev were included in the present phase-shift analysis, except the well-known narrow $7/2^-$ level at $E_p=3.47$ Mev and narrow levels at proton energies of 7.180, 7.280, 7.287, and 7.305 Mev. These latter levels may be considerably narrower than our experimental resolution. This likelihood together with the possibility of strong damping from open channels discouraged us from attempting an analysis of these narrow resonances. For these, and for all levels above $E_p=7.385$ Mev, the resonant energy and upper limits on the lab width were estimated by inspection.

Figure 11 shows a comparison of the energy level structure of O^{17} and F^{17} . Dashed lines connect levels in O^{17} and F^{17} having the same total angular momentum and parity and similar resonant energies and reduced widths.

A one-to-one correspondence is found for all levels up to the $E_x=5.23$ Mev level in O^{17} . This 5.23-Mev level in O^{17} is not seen by $(O^{16}+n)$ so presumably has a very small nucleon width. The $1/2^+$ and the $3/2^+$ levels at $E_x=5.68$ and 5.82 Mev, respectively, in F^{17} could correspond to unassigned levels in O^{17} at $E_x=5.73$ and 5.87 Mev. The former is not seen in neutron scattering so has a very small nucleon width. This small width suggests correspondence to the $1/2^+$ at $E_x=5.68$ Mev in F^{17} whose width is just measurable. The level in O^{17} at $E_x=5.87$ Mev has an angular momentum $\geq 3/2$ according to neutron work, so likely corresponds to our $3/2^+$ level at $E_x=5.82$ Mev in F^{17} .

Above $E_x=6$ Mev there is only a very rough agreement in level density. Two levels out of the five in this region for which we have F^{17} assignments have known corresponding levels in O^{17} .

Interpretation of F^{17} Level Structure

It is of interest to attempt a crude shell-model interpretation of the presently observed low states of F^{17} . We may first, following Lane,¹⁴ consider the "normal"-parity states ("normal" meaning the same as the ground state).

Normal-Parity States

Figure 12 shows the identified normal-parity states below $E_x=7.5$ Mev. The large reduced widths of the first three states, $5/2$, $1/2$, $3/2$, require that these be nearly pure single-particle states corresponding to a $1d_{5/2}$, a $2s_{1/2}$, and a $1d_{3/2}$ particle plus an O^{16} core: i.e., $(O^{16})_{0+} \times 1d_{5/2}$, etc., where $(O^{16})_{0+} \times 0$ corresponds to $(1s^4 1p^{12})_0$ and \times denotes vector coupling. The $1d_{5/2}-2s_{1/2}$ spacing is, therefore, fixed at ~ 0.5 Mev and the $d_{5/2}-d_{3/2}$ splitting as 5.1 Mev.

It is, then, tempting to see how closely one can account for the higher levels in terms of known excited states of O^{16} as parents of the F^{17} states. The only low

states of O^{16} , which can couple to $2s$ or $1d$ orbitals for the normal-parity F^{17} states, are the 0^+ state at 6.06 Mev and the 2^+ state at 6.92 Mev.

The states of such parentage and their predicted energies are indicated also in Fig. 12. Comparison with observation shows the following interesting features: a $1/2^+$ state of moderate reduced width occurs precisely at the energy predicted by $(O^{16})_{0+} \times 2s_{1/2}$ (i.e., 6.06 Mev above the $(O^{16})_{0+} \times 2s_{1/2}$ single-particle state). In addition, a $3/2^+$ state of moderate width occurs at $E_x=7.48$ Mev which is almost exactly the 7.42-Mev energy again expected from $(O^{16})_{2+} \times 2s_{1/2}$. In the latter case, a $5/2^+$ level is also predicted but not observed; however, two $5/2$ levels, parity unknown, are seen near this energy in the mirror nucleus O^{17} (see Fig. 11).

The states expected from $(O^{16})_{0+} \times 1d_{5/2}$ and $(O^{16})_{2+} \times 1d_{5/2}$ do not correspond so well with the experiment. However, if the coupling of these O^{16} states to the $1d_{5/2}$ particle were to result in small reduced widths, qualitative agreement is obtained. Notice that the two states of smallest reduced width ($1/2^+$ at $E_x=5.68$ and $3/2^+$ at $E_x=6.78$) would be from these couplings. Since such small reduced widths were just on the experimental limit of detection, it would, therefore, not be surprising if the other predicted states are undetected. This is *a fortiori* true for the $J=7/2$, $9/2$ states, where the laboratory width is further reduced by the large centripetal barrier ($l=4$ or 6 is required to form the state). The main puzzle remaining would be the unpredicted $3/2^+$ level at $E_x=5.82$ Mev, which is observed to be of moderate reduced width.

An alternate and partly equivalent way of viewing the problem is to examine the lowest F^{17} states which can be generated by promoting two p nucleons to s or d orbits. If the lowest states always arise from coupling pairs of equivalent particles to zero angular momentum, then the lowest configurations give

$$(1p^{-2})_0(1d_{5/2}^3)_{5/2} \rightarrow J=5/2^+, \quad (1)$$

$$(1p^{-2})_0(1d_{5/2}^2)_0(2s_{1/2}) \rightarrow J=1/2^+, \quad (2)$$

$$(1p^{-2})_0(2s_{1/2}^3)_{1/2} \rightarrow J=1/2^+, \quad (3)$$

$$(1p^{-2})_0(2s_{1/2}^2)_0(1d_{5/2}) \rightarrow J=5/2^+, \quad (4)$$

and possibly

$$(1p^{-2})_0(1d_{5/2}^2)_0(1d_{3/2}) \rightarrow J=3/2^+, \quad (5)$$

$$(1p^{-2})_0(2s_{1/2}^2)_0(1d_{3/2}) \rightarrow J=3/2^+. \quad (6)$$

The above scheme predicts two, and only two, $1/2^+$ excited states of F^{17} . This result is in accord with observation. In addition, the experimental energy gap between these two states is nearly 1 Mev which agrees with the configuration prediction, since the two states from (2) and (3) differ only in promoting two $d_{5/2}$ nucleons to the $2s_{1/2}$ orbit. (The cost per nucleon is 0.5

¹⁴ A. M. Lane, Revs. Modern Phys. **32**, 519 (1960).

Mev, according to the observed $1d_{5/2}-2s_{1/2}$ difference of the single-particle states.) The above scheme predicts two unobserved $5/2^+$ states and is still deficient in accounting for one of three observed $3/2^+$ states, which lie above the 5.1-Mev single-particle $d_{3/2}$ state. These weaknesses can be largely corrected by supposing that the three $d_{5/2}$ nucleons of configuration (1) couple to $3/2$ instead of $5/2$. This type coupling ($J=j-1$) is in agreement with the fact that three $d_{5/2}$ nucleons are known to couple to $3/2^+$ for the ground states of Ne²¹ and Na²³. An alternate method of generating the missing $3/2^+$ state would be to consider a four-hole configuration and a quasi-alpha particle coupled to the $1d_{3/2}$ orbital. Thus,

$$(1p^{-4})_0(2s_{1/2}^4)(1d_{3/2}) \quad (7)$$

might, because of the quasi-alpha particle structure, lie low enough to be considered. If one of the $3/2^+$ state is of this character, the width for the α channel (which opens at $E_x=5.8$ Mev) might be anomalously large. Current O¹⁶(p,α)N¹³ measurements at Wisconsin may check this.

Non-Normal-Parity States of F¹⁷ (i.e., odd parity)

No odd-parity states of large reduced width are seen among the identified levels. There is some evidence for a very broad $3/2^-$ level above $E_x=7.5$ Mev although the analysis was not carried to high enough energy to unambiguously identify it. However, since in the mirror nucleus, O¹⁷, a single-particle $3/2^-$ state has been seen near this energy we will tentatively assume that our broad unidentified level at $E_x=7.7$ Mev is indeed the $2p_{3/2}$ single-particle state of F¹⁷.

If we again try to associate the remaining F¹⁷ states in terms of O¹⁶ excited parent states, we do not find even qualitative agreement. The relevant O¹⁶ excited states are the second and fourth, the 3^- at 6.14 Mev and the 1^- at 7.12 Mev.

If we adopt the alternate gambit of promoting odd numbers of p nucleons to $1d$ or $2s$ orbitals, one is in equal difficulty to generate the correct number of states and to account for the energies in terms of rather pure simple configurations.

It seems clear then that for the odd-parity states there is strong mixing of configurations. Lane¹⁴ attempts to include, empirically, these effects by starting with the observed states of F¹⁸ as parents and then coupling these to a $p_{1/2}$ hole. Unfortunately, F¹⁸ has a plethora of poorly identified low-lying states so this procedure tends to be ambiguous and the energetics are not convincing. Even more objectionable is the fact that the first $T=1$ state of F¹⁸ occurs within 1 Mev of the ground state, whereas the corresponding $T=3/2$ state of F¹⁷ lies at least 5 Mev higher than the region we are considering.

It seems more reasonable that these odd-parity states involve the promotion of three p nucleons to s and d orbits. The parent nucleus which might empirically best include the configuration mixing would then be Ne²⁰. We attempt to generate the non-normal F¹⁷ state by coupling the Ne²⁰ states to three p holes. The results are shown in Fig. 12, where for purposes of comparison the lowest predicted $1/2^-$ state has been normalized to the lowest observed $1/2^-$ state. Some agreement is noted. A $3/2^-$ state is predicted at $E_x=4.74$ Mev and a $7/2^-$ state at 7.35 Mev, both of which are close in energy to observed $3/2^-$ and $7/2^-$ states. The predicted $5/2^-$ may be the unidentified but small nucleon width level seen in O¹⁷ at $E_x=5.22$ Mev and unobserved in F¹⁷, because of the expected small lab width. The missing $9/2^-$ level would also have too small a lab width to be detected. Left unaccounted for are, however, two other $7/2^-$ states, three other $3/2^-$ states, and one other $1/2^-$ state. One could generate a number of these observed states by permitting the three ($p_{1/2}$) holes to couple to $3/2^-$, but energetics are unconvincing and the model has lost its simplicity.

Giant Resonance Interpretation

The relative abundance of $3/2^+$, $7/2^-$, and $3/2^-$ states and the complete absence of unbound $5/2^+$ and $5/2^-$ states may be partially misleading, since systematic differences in reduced widths for these states would favor the experimental detection of that class of states with the systematically larger width. In fact, according to the giant resonance interpretation of Lane, Thomas, and Wigner,¹⁵ there should be a marked enhancement of γ^2 for levels of a given J^π , when these energies are close to the corresponding single-particle states. In the present case, the single-particle $d_{3/2}$ state is well within the region of observation while the $d_{5/2}$ single-particle state (the ground state) lies 5 Mev below. The $2p_{3/2}$ state is believed just beyond the experimental region and the $f_{7/2}$ state is certainly expected to be ~ 5 Mev closer than the $f_{5/2}$. The $5/2^+$ and $5/2^-$ states predicted in Fig. 12 may, hence, have been missed simply because their unenhanced γ^2 give lab widths below the detection level. On the other hand, $1/2^\pm$ states are experimentally observed in the absence of nearby single-particle states. However, the small barrier for these states does permit smaller γ^2 to be experimentally detected.

APPENDIX

In the case of branching solutions, proper selection was sometimes very difficult. It was usually necessary to pursue both solutions until the fit, (i.e., χ^2) of one becomes clearly inadequate or the variation of one set of phase shifts with energy becomes anomalous.

¹⁵ A. M. Lane, R. G. Thomas, and E. P. Wigner, Phys. Rev. 98, 693 (1955).

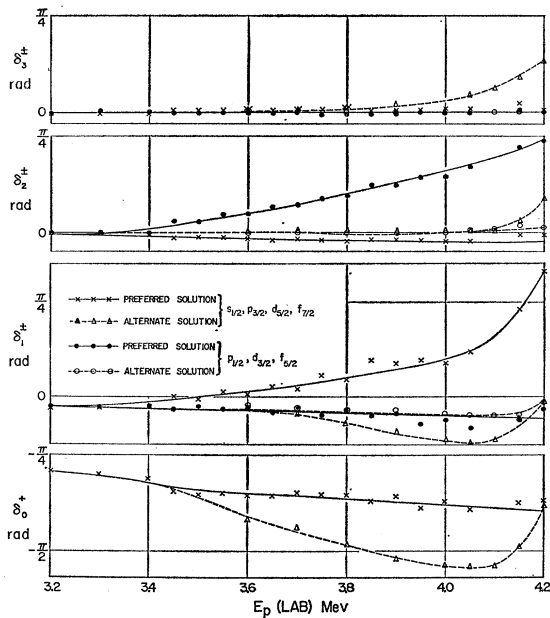


FIG. 13. Illustration of branching solutions in the low-energy region. The solid and dashed lines are smooth curves showing the general behavior of the preferred and alternate solutions, respectively.

We will give two illustrations of branching solutions. These are not the only cases of branching that were found. However, they are the cases in which picking a preferred solution was the most difficult.

(1) Branching in the $E_p = 3.4$ to 4.2 Mev region. (See Fig. 13.) The preferred and alternate solutions begin to branch at about 3.4 Mev and differ only in the following ways:

(a) As the proton energy approaches 4.2 Mev, the alternate solution implies resonances in the δ_0^+ , δ_1^+ , δ_1^- , δ_2^+ , and δ_3^+ phase shifts. The preferred solution implies resonances only in the δ_1^+ and δ_2^- phase shifts. The preferred solution implies no other resonances until about 4.7 Mev. Inspection of the cross sections in this region shows only two maxima and minima implying only two levels.

(b) χ^2 for the preferred solution ranges from 10 to 30. For the alternate solution, χ^2 is initially the same, but rises continuously to 300 at 4.2 Mev. $\chi^2 = 8$ indicates fit within assigned errors.

(2) Branching in the $E_p = 5.7$ to 6.6 Mev region. (See Fig. 14.) Our neglect of possible opening channels makes it more difficult to exclude alternate solutions

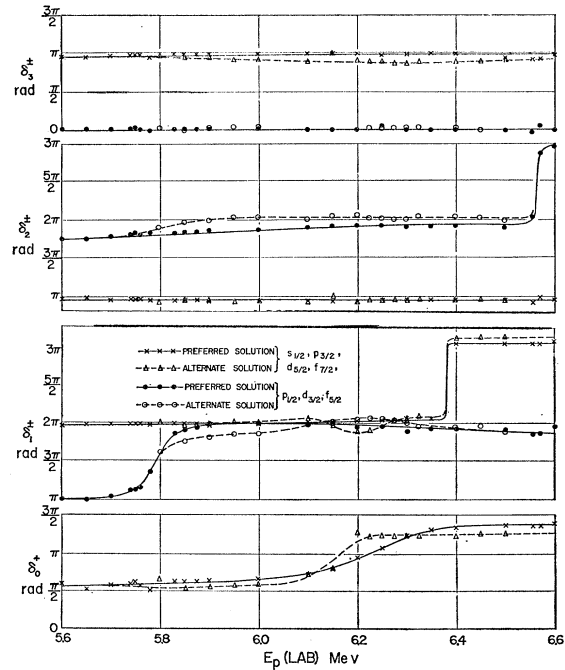


FIG. 14. Branching solutions in the region about $E_p = 6$ Mev. The solid and dashed lines are smooth curves showing the general behavior of the preferred and alternate solutions, respectively.

on the basis of "normal" resonant behavior of the phase shifts. The solutions begin to branch at $E_p = 5.7$ Mev and differ only in the following ways:

(a) The alternate solution gives an anomalous behavior for the δ_1^- phase shift for the resonance at $E_p = 5.83$ Mev. This phase shift lacks $\pi/4$ radians of its expected resonant change. The level is not broad, and the p -wave penetrability is nearly constant so there is no obvious explanation of this behavior. The preferred solution, however, acts normally in this region.

(b) In the region of 5.9 Mev, the δ_2^- phase shift has an unphysical lump in the alternate solution. For the preferred solution, it behaves normally.

(c) Neither the alternate nor the preferred solution for the δ_0^+ phase shift change by π radians in traversing the resonance at $E_p = 6.3$ Mev. However, the discrepancy is much worse in the case of the alternate solution.

(d) In the region of $E_p = 6.3$ Mev the δ_1^- phase shift acts like a normal potential phase shift for the preferred solution. For the alternate solution the δ_1^- phase shift has a well-defined lump around $E_p = 6.2$ Mev.